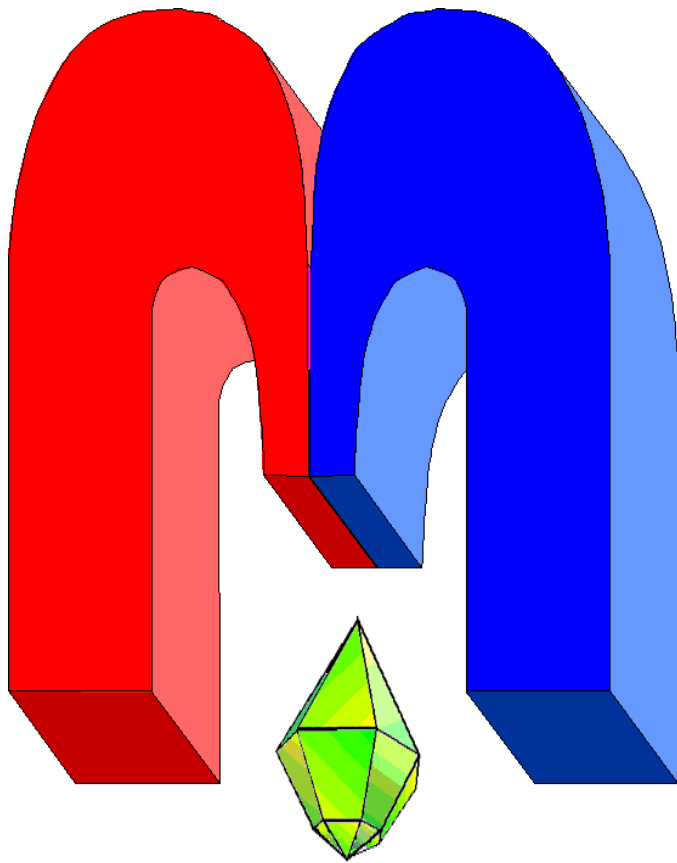


ISSN 2072-5981

doi: 10.26907/mrsej



***Magnetic
Resonance
in Solids***

Electronic Journal

Volume 21

Issue 2

Paper No 19205

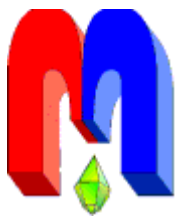
1-7 pages

2019

doi: 10.26907/mrsej-19205

<http://mrsej.kpfu.ru>

<http://mrsej.ksu.ru>



Established and published by Kazan University
Endorsed by International Society of Magnetic Resonance (ISMAR)
Registered by Russian Federation Committee on Press (#015140),
August 2, 1996
First Issue appeared on July 25, 1997

© Kazan Federal University (KFU)*

"Magnetic Resonance in Solids. Electronic Journal" (MRSej) is a peer-reviewed, all electronic journal, publishing articles which meet the highest standards of scientific quality in the field of basic research of a magnetic resonance in solids and related phenomena.

Indexed and abstracted by
Web of Science (ESCI, Clarivate Analytics, from 2015), Scopus (Elsevier, from 2012), RusIndexSC (eLibrary, from 2006), Google Scholar, DOAJ, ROAD, CyberLeninka (from 2006), SCImago Journal & Country Rank, etc.

Editor-in-Chief

Boris **Kochelaev** (KFU, Kazan)

Honorary Editors

Jean **Jeener** (Universite Libre de Bruxelles, Brussels)


Raymond **Orbach** (University of California, Riverside)

Executive Editor

Yurii **Proshin** (KFU, Kazan)
mrsej@kpfu.ru



This work is licensed under a [Creative Commons Attribution-ShareAlike 4.0 International License](https://creativecommons.org/licenses/by-sa/4.0/).

 This is an open access journal which means that all content is freely available without charge to the user or his/her institution. This is in accordance with the [BOAI definition of open access](#).

Technical Editor

Alexander **Kutuzov** (KFU, Kazan)

Editors

Vadim **Atsarkin** (Institute of Radio Engineering and Electronics, Moscow)

Yurij **Bunkov** (CNRS, Grenoble)

Mikhail **Eremin** (KFU, Kazan)

David **Fushman** (University of Maryland, College Park)

Hugo **Keller** (University of Zürich, Zürich)

Yoshio **Kitaoka** (Osaka University, Osaka)

Boris **Malkin** (KFU, Kazan)

Alexander **Shengelaya** (Tbilisi State University, Tbilisi)

Jörg **Sichelschmidt** (Max Planck Institute for Chemical Physics of Solids, Dresden)

Haruhiko **Suzuki** (Kanazawa University, Kanazawa)

Murat **Tagirov** (KFU, Kazan)

Dmitrii **Tayurskii** (KFU, Kazan)

Valentine **Zhikharev** (KNRTU, Kazan)

* In Kazan University the Electron Paramagnetic Resonance (EPR) was discovered by Zavoisky E.K. in 1944.

Influence of structure effects and orbital ordering on the magnetic hyperfine field in pyrochlore oxides $R_2V_2O_7$ ($R = \text{Lu}, \text{Yb}, \text{Tm}, \text{Er}, \text{Ho}$): *ab initio* calculations

P.A. Agzamova

M.N. Miheev Institute of Metal Physics of Ural Branch of Russian Academy of Sciences,
S. Kovalevskaya str. 18, Ekaterinburg 620108, Russia
Ural Federal University, Mira str. 19, Ekaterinburg 620002, Russia

E-mail: polly@imp.uran.ru

(Received March 19, 2019; revised May 27, 2019;
accepted May 28, 2019; published June 14, 2019)

The detailed *ab initio* calculations of crystal structure and hyperfine interaction parameters are presented for $R_2V_2O_7$ system ($R = \text{Ho}, \text{Er}, \text{Tm}, \text{Yb}, \text{Lu}$) to investigate the effect of the V-ion environment due to R -ion substitution on the local magnetic properties of ^{51}V nucleus. It is shown that this effect is very small, but the orbital ordering dictates a large anisotropy of magnetic hyperfine tensor in $R_2V_2O_7$ system.

PACS: 71.15.Mb, 71.20.Be, 74.25.nj, 75.25.Dk, 75.47.Lx.

Keywords: density functional theory, hyperfine interactions, NMR, orbital ordering, pyrochlores.

1. Introduction

Orbital degrees of freedom and its interplay with lattice and spin ones play the major role in strongly correlated systems and generate the complex electrical and magnetic properties of transition metal oxides.

In the last few years the geometrically frustrated systems have attracted much interest as materials demonstrating new orbital states such as orbital liquid or spin-orbital liquid and so on [1, 2]. Among these systems the rare-earth vanadate pyrochlores ($R_2V_2O_7$) have provided additional interest, since the V^{4+} ions, located in the pyrochlore lattice, are the orbital degenerate ions, and its orbital ordering is interesting from the viewpoint of its specific geometrical structure. In addition, some important features of magnetic behavior of vanadate pyrochlores are surprising. For instance, compounds with $R = \text{Y}, \text{Er}, \text{Tm}, \text{Yb}, \text{Lu}$ are reported to be ferromagnetic insulators as opposed to usually observed the metallic state [3, 4]. Furthermore, $\text{Lu}_2\text{V}_2\text{O}_7$ and $\text{Ho}_2\text{V}_2\text{O}_7$ have attracted great interest due to the magnon Hall effect [5, 6].

Our work was initially stimulated by investigations of orbital ordering in transition metal oxides with orbital degeneracy by the nuclear magnetic resonance (NMR) method [7-9]. The NMR spectra are determined by electric quadrupole and magnetic dipole hyperfine interactions. The electric quadrupole hyperfine interaction is the interaction between the nuclear quadrupole moment and electron one, and characterized by the quadrupole frequency. The magnetic hyperfine interaction is the interaction between nuclear and electronic magnetic moments. It contains isotropic and anisotropic terms. The latter depends on the orbital ordering of magnetic ions.

In some cases, for instance, in titanates, where Ti^{3+} ion is located within the oxygen octahedron, the R -ion displacement effects on the t_{2g} -level splitting, and the change of the $3d$ orbital state of Ti^{3+} ions is observed [10]. The similar situation can be expected in rare-earth vanadate pyrochlores.

The change of $3d$ orbital state due to R -ion displacement can favour further changes of the unpaired spin density on magnetic ion nucleus. This effect may occur owing to the interplay between the orbital state of $3d$ -shell and the local environment distortion. The $3d$ -shell modification initiates changes of the s -polarization and further changes of the unpaired spin density on nucleus, and, moreover, can give rise to changes of the spin density distribution around nucleus. These effects can influence on isotropic and anisotropic hyperfine interaction values.

There are two approaches to obtain the hyperfine coupling constant. The first one is the *ab initio* approach, where we optimized the crystal structure of compounds during self-consistent calculation and evaluated the hyperfine coupling constants. The second one is the model approach in the framework of the crystal field theory. Here, *i*) we analyzed the magnetic hyperfine interaction Hamiltonian leaning upon known orbital structure data and obtained the angular dependences of NMR spectrum under the external magnetic field for each V ion; *ii*) we could derive the information about hyperfine interaction values leaning upon the experimental data of NMR resonance frequencies [9]. Such calculations have been performed for $\text{Lu}_2\text{V}_2\text{O}_7$ [11, 12]. We compared data from *ab initio* and model approaches and found a good agreement between them. It allowed us to conclude that the first-principles calculations are suitable to obtain the information about isotropic and anisotropic hyperfine coupling constants in the absence of NMR experimental data.

So, the aim of present work is to clarify the influence of structure effects and orbital ordering on the magnetic hyperfine field in pyrochlore oxides $R_2\text{V}_2\text{O}_7$ ($R = \text{Lu}, \text{Yb}, \text{Tm}, \text{Er}, \text{Ho}$) in the absence of experimental values of the NMR resonance frequencies by the detailed *ab initio* calculations of the hyperfine parameters.

2. Methods

Ab initio calculations

Optimization of the crystal structure and calculations of the hyperfine interaction parameters for $R_2\text{V}_2\text{O}_7$ have been carried out by using hybrid functional PBE0 [13, 14] within framework of MO LCAO (molecular orbitals as linear combination of atomic orbitals) approach with the periodic CRYSTAL14 code [15]. Exchange-correlation functional is known to yield better agreement between the calculated and experimental electronic and magnetic properties of solids [16, 17].

The PBE0 functional contains a mixture of exact Hartree-Fock exchange, controlled by a parameter, and DFT exchange-correlation term. Usually a parameter equals 0.25 but it is important to use the Hartree-Fock exchange equaled 1 for calculations of the local hyperfine parameters.

On the first step the self-consistent calculation of the wave functions has been carried out with using the same all-electron Gaussian basis sets for oxygen [18] and vanadium [19] ions for $R_2\text{V}_2\text{O}_7$ compounds, and quasi-relativistic effective-core pseudopotentials (ECP) for rare-earth ions, where the $4f$ -orbitals were replaced by a pseudopotential known as $4f$ -in-core ECP. The ECPs and corresponding valence basis sets are available at the online repository [20].

On the second step we have used the calculated wave functions to evaluate the isotropic and anisotropic hyperfine coupling constants.

Hyperfine interaction parameters

The magnetic hyperfine interaction Hamiltonian (H_{hf}), adopted in this work, couples electron and nuclear magnetic spins, \mathbf{S} and \mathbf{I} , via [21]

$$H_{\text{hf}} = \mathbf{I} \cdot \mathbf{A} \cdot \mathbf{S}. \quad (1)$$

The coupling constant \mathbf{A} contains both an isotropic term

$$A_{\text{iso}} = \frac{2\mu_0}{3h} g_e \mu_B g_N \mu_N \rho_S(0), \quad (2)$$

and an anisotropic term

$$A_{\text{an}} = \frac{2\mu_0}{3h} g_e \mu_B g_N \mu_N \rho_S \left[T_{11} - \frac{1}{2}(T_{22} + T_{33}) \right], \quad (3)$$

where μ_0 is the vacuum susceptibility, g_e and g_N are the electron and nuclear g -factors, μ_N is the nuclear magneton, h is Planck's constant, $\rho_S(0)$ is the electron spin density at the nucleus, T_{ii} are the principal components of the anisotropic hyperfine coupling tensor \mathbf{T} , which depends on the electron structure of the system. The \mathbf{T} tensor is a second-rank symmetric 3×3 tensor defined as a quadrupole moment of the spin density at V ion position (ρ_S). The \mathbf{T} tensor components are defined as

$$T_{ij} = \sum_{\mu\nu\sigma} P_{\mu\nu\sigma} \int d\mathbf{r} \phi_{\mu\sigma}(\mathbf{r}) \left(\frac{r^2 \delta_{ij} - 3x_i x_j}{r^5} \right) \phi_{\nu\sigma}(\mathbf{r}). \quad (4)$$

T tensor [21] in this work is calculated using the full spin-polarized density matrix $P_{\mu\nu\sigma}$ and Bloch basis functions $\phi_{\mu\sigma}$. Spin-orbit coupling is not included in the Hamiltonian. The sum over single-electron spins σ in Eq. (4) means that the spin **S** is a spin-half operator in a quantized form of Eq. (1). When **A** is isotropic with positive diagonal elements A_{iso} and **I** and **S** are spin-half operators, H_{hf} has a singlet ground state and a triplet excited state lying A_{iso} above the ground state.

The electric hyperfine interaction is characterized by the quadrupole frequency

$$\nu_Q = \frac{3eQ_N |V_{ZZ}|}{2I(2I-1)\hbar}, \quad (5)$$

where Q_N is the nuclear quadrupole moment, V_{ZZ} represents the component of the electric field gradient (EFG) tensor in the principal axes ($|V_{XX}| \leq |V_{YY}| \leq |V_{ZZ}|$). In general case, the principal axes of **T** tensor and EFG tensor can be different.

3. Results and discussions

Crystal structure

The pyrochlore $R_2V_2O_7$ crystallizes into a face centered cubic structure with eight formula units in a unit cell and the $Fd\bar{3}m$ space group symmetry [22]. The Wyckoff positions and fractional positions of ions in the unit cell are $R(16d) - (0.5, 0.5, 0.5)$, $V(16c) - (0, 0, 0)$, $O(48f) - (x, 0.125, 0.125)$, $O'(8b) - (0.375, 0.375, 0.375)$ respectively.

The crystal structure of rare-earth vanadate pyrochlore is characterized as a three dimensional network of corner-sharing coordination tetrahedra of either *R*- and *V*-ions (fig. 1a). The *R* ions are eight-fold coordinated by oxygen ions and located within distorted cubes (fig. 1b). The *V* ions are six-fold coordinated by oxygen ions and located within octahedra deformed along C_3 axis (fig. 1c). There are two non-equivalent positions of oxygen ions.

At the first step, we have optimized the crystal structures for rare-earth vanadates to investigate the modification of V^{4+} ion lattice environment due to the *R*-ions substitution. The results of full geometry optimization of lattice parameters and bond lengths are collected in Table 1.

The calculated lattice parameters are smaller than the experimental ones with a difference about 2%. Therefore, the optimized lattice parameters of $R_2V_2O_7$ system calculated with PBE0 functional and valence basis set included polarization *f*-functions describe the crystal structures in good agreement with experiment [23, 24].

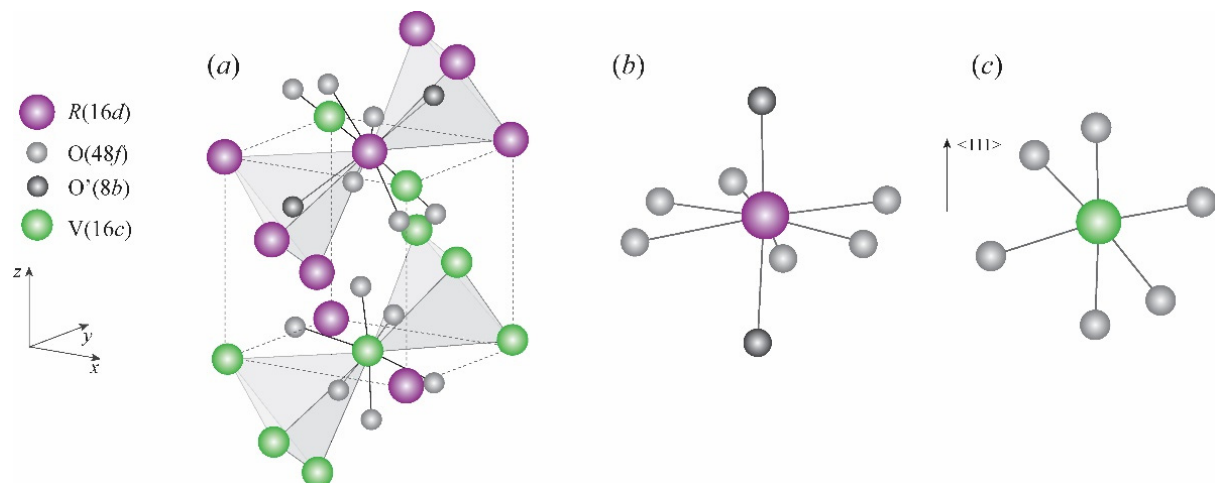
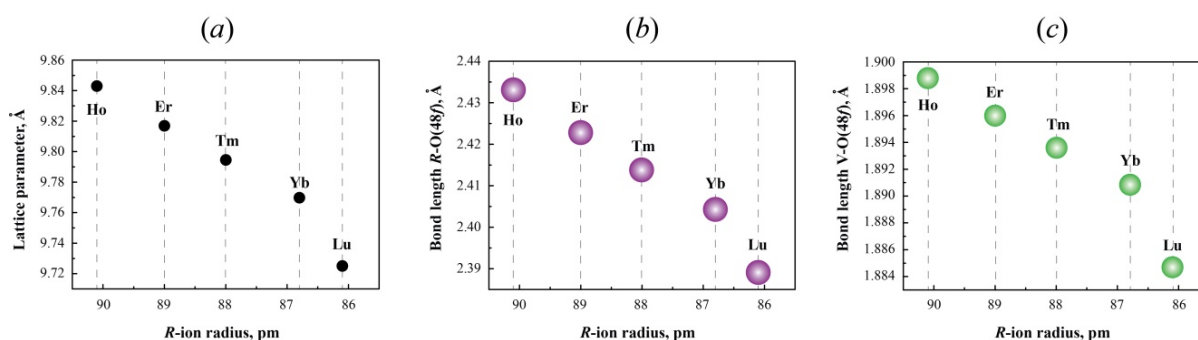


Figure 1. (a) Crystal structure of $R_2V_2O_7$ system; (b) *R*-ion environment; (c) *V*-ion environment.

Table 1. Calculated lattice constant, bond-length $R\text{-O}(48f)$, bond-length $V\text{-O}(48f)$ compared with experimental data: for $\text{Ho}_2\text{V}_2\text{O}_7$ and $\text{Er}_2\text{V}_2\text{O}_7$ – [23]; for $R_2\text{V}_2\text{O}_7$ with $R = \text{Tm}, \text{Yb}, \text{Lu}$ – [24].

R	Lattice parameter (Å)		$R\text{-O}(48f)$ (Å)		$V\text{-O}(48f)$ (Å)	
	Calc.	Exp.	Calc.	Exp.	Calc.	Exp.
Ho	9.843	9.999	2.433	–	1.899	–
Er	9.817	9.998	2.423	–	1.896	–
Tm	9.795	9.973	2.414	2.445	1.894	1.936
Yb	9.770	9.945	2.404	2.438	1.891	1.930
Lu	9.725	9.928	2.389	2.426	1.885	1.931


Figure 2. Calculated lattice constant (a), bond length $R\text{-O}(48f)$ (b), and bond length $V\text{-O}(48f)$ (c).

In Figure 2 it is shown the decreasing of the lattice parameters in relation to the rare-earth ion, which is according to the lanthanide contraction.

Let us consider the change in the distances $R\text{-O}$ and $V\text{-O}$. Distances $R\text{-O}(48f)$ and $V\text{-O}(48f)$ decrease in series $R = \text{Ho}$ to Lu as the radius of the lanthanide decreases. The $V\text{-O}$ bond length is changed about 0.01 \AA across the series. The difference is very small to observe some effect of R -ions displacement on the V^{4+} lattice environment modification. As a result, we cannot expect changes of the orbital ordering across series and therefore we could not obtain any changes of hyperfine interaction constants for all compounds.

Hyperfine interaction parameters

The nuclear magnetic resonance spectrum is determined by the hyperfine interaction Hamiltonian

$$\hat{H}_{\text{HF}} = \hat{H}_{\text{el}} + \hat{H}_{\text{mag}}. \quad (6)$$

Here the first term is the electric quadrupole hyperfine interaction Hamiltonian; the second one is the magnetic hyperfine interaction Hamiltonian.

The electrostatic hyperfine interaction is characterized by the quadrupole frequency ν_Q (3). It should be noted that the quadrupole frequency $i)$ decreases in series $R = \text{Ho}$ to Lu as the radius of lanthanide decreases; $ii)$ is rather small in comparison with the magnetic hyperfine coupling constants (see fig. 3a). Such small value of the quadrupole frequency is in agreement with the experimental one [9] and the expected one of about 1 MHz for ^{51}V nuclei in a d^1 state [25-27]. Therefore, we can conclude that the local properties of ^{51}V nuclei in $R_2\text{V}_2\text{O}_7$ system are determined mainly by the magnetic hyperfine interaction.

The magnetic hyperfine interaction is characterized by the isotropic hyperfine coupling constant A_{iso} (2) and the anisotropic hyperfine coupling constant A_{an} (3). In this work we have performed *ab initio* calculations of A_{iso} and A_{an} for the ^{51}V nucleus in $R_2\text{V}_2\text{O}_7$ system. The results are presented in Figure 3(b,c). The calculations have been performed with making use of the following constant values (in SI system): $g_{\text{N}} = 1.46837$, $I = 7/2$, $Q_{\text{N}} = 4 \times 10^{-26} \text{ cm}^2$ [28].

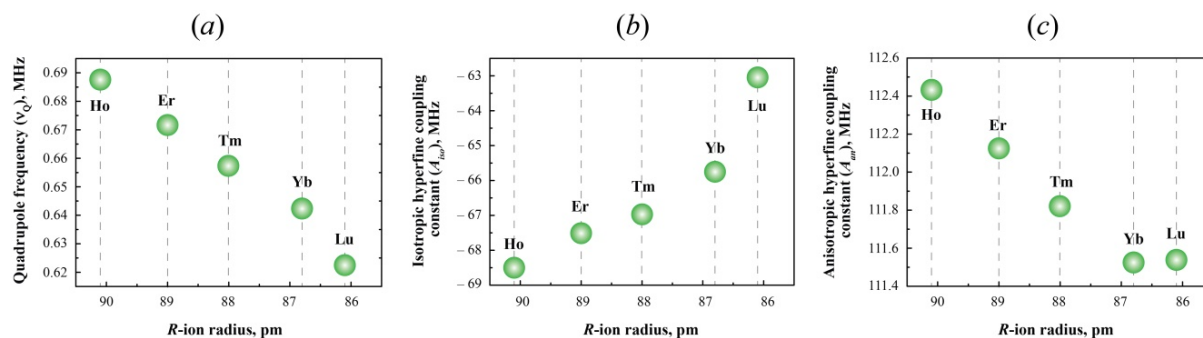


Figure 3. Calculated quadrupole frequency (ν_Q) (a), the isotropic hyperfine coupling constant (A_{iso}) (b), and the anisotropic hyperfine coupling constant (A_{an}) (c) for $R_2V_2O_7$ ($R = \text{Ho, Er, Tm, Yb, Lu}$).

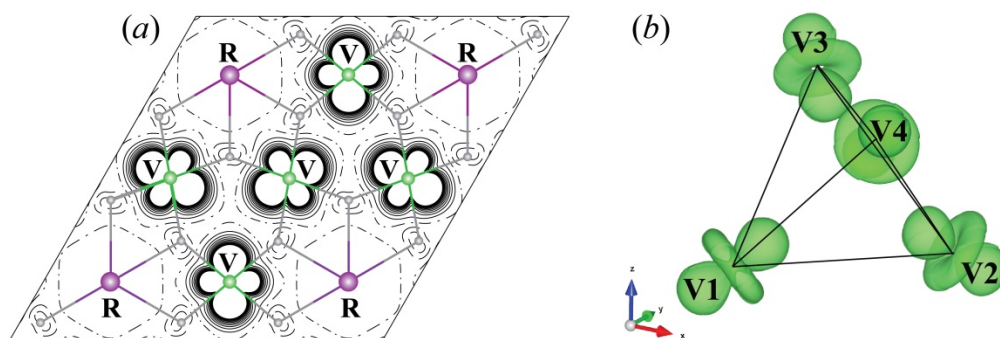


Figure 4. Calculated spin density maps for $R_2V_2O_7$ system: (a) 2D spin density map plotted in (111) plane (solid line – positive spin density values, dashed line – negative spin density values, dash-dotted line – zero spin density value); (b) 3D spin density map.

The absolute value of the isotropic hyperfine coupling constant decreases in series $R = \text{Ho}$ to Lu (see fig. 3b) as the bond lengths $\text{V-O}(48f)$ and $\text{R-O}(48f)$ decrease (see fig. 2b,c). The isotropic hyperfine interaction depends on the local environment of vanadium ion. Our *ab initio* calculations showed that the decreasing of R -ions radius leads to slight changes of bond lengths between V^{4+} ion and surrounding oxygen atoms (see fig. 2c). Therefore, such slight modifications of the vanadium local environment lead to the small changes of the isotropic hyperfine coupling constants about 6 MHz.

The same situation is observed in the case of *ab initio* calculations of the anisotropic hyperfine coupling constant, where the difference between A_{an} for $\text{Ho}_2V_2O_7$ and $\text{Lu}_2V_2O_7$ is about 1 MHz (fig. 3c). The anisotropic hyperfine interaction is directly connected with the quadrupole moment of vanadium ion. The latter is the order parameter for orbital degree of freedom. Small changes of anisotropic hyperfine coupling constant in series $R = \text{Ho}$ to Lu give us evidence for the absence of significant changes of the orbital ordering in $R_2V_2O_7$ system.

It is very important to have the information about spin density distribution around ^{51}V nucleus. We can obtain it from the spin density maps. These maps plotted from *ab initio* calculations are similar in series $R = \text{Ho}$ to Lu and presented in Figure 4.

The plotted spin density maps demonstrate d_{22} -type (in local coordinate frame) of the spin density distribution around vanadium nucleus that agrees with *i*) expected type for t_{2g}^1 electronic configuration in octahedral complex, when orbitals are directed along C_3 -axis; *ii*) experimental type observed by NMR [9] and neutron polarized diffraction [29] techniques.

In spite of very small changes of the magnetic hyperfine interaction parameters due to small modifications of V -ion environment in $R = \text{Ho}$ to Lu series the anisotropy of hyperfine interactions for the vanadium ion nucleus is rather large. Usually the anisotropic hyperfine interaction is very small and neglected at description of nuclear magnetic resonance spectra of $3d$ -ions. It was shown above that the anisotropic part of magnetic hyperfine interaction depends on orbital degree of freedom directly.

It allows us to conclude that the orbital ordering determines a large anisotropy of magnetic hyperfine fields in $R_2V_2O_7$. This result agrees with our earlier studies of $Lu_2V_2O_7$ in the framework of model and *ab initio* approaches [11, 12] and experimental investigations of $Lu_2V_2O_7$ by NMR method [9]. At present there are no any experimental and theoretical data for other compounds in $R_2V_2O_7$ series.

4. Summary

In summary, we can conclude that *i*) the substitution of R -ions in $R_2V_2O_7$ system has slight effect on the modification of the V^{4+} lattice environment; *ii*) the orbital ordering does not change in $R = Ho$ to Lu series; *iii*) the orbital ordering dictates a large anisotropy of magnetic hyperfine tensor for $R_2V_2O_7$ system with $R = Lu, Yb, Tm, Er, Ho$.

Acknowledgments

I would like to thank professor E.V. Mostovshchikova and professor M.I. Kurkin for fruitful discussions. This work was performed using «Uran» supercomputer of IMM UB RAS in the framework of the State Task of the FASO of the Russian Federation (theme “Diagnostics”, no. AAAA-A18-118020690196-3) and was supported in part by the RFBR no. 18-32-00690.

References

1. Dun Z.L., Garlea V.O., Yu C., Ren Y., Chou E.S., Zhang H.M., Dong S., Zhou H.D. *Phys. Rev. B* **89**, 235131 (2014)
2. Scoulatos M., Toth S., Roessli B., Enderle M., Stunault F., McIntyre G.J., Tung L.D., Majerison C., Pomjakushina E., Brown P.J., Khomskii D.I., Rüegg Ch., Kreyssig A., Goldman A.I., Goff J.P. *Phys. Rev. B* **91**, 161104 (2015)
3. Soderholm L., Greedan J.E. *Mag. Res. Bull.* **17**, 707 (1982)
4. Ali Biswas A., Jana Y. *JMMM* **329**, 118 (2013)
5. Onose Y., Ideue T., Katsura H., Shiomi Y., Nagaosa N., Tokura Y. *Science* **329**, 297 (2010)
6. Ideue T., Onose Y., Katsura H., Shiomi I., Ishiwata S., Nagaosa N., Tokura Y. *Phys. Rev. B* **85**, 134441 (2012)
7. Kiyama T., Itoh M. *Phys. Rev. B* **91**, 167202 (2003)
8. Kiyama T., Saitoh H., Itoh M., Kodama K., Ichikawa H., Akimitsu J. *J. Phys. Soc. Jap.* **74**, 1123 (2005)
9. Kiyama T., Shiraoka T., Itoh M., Kano L., Ichikawa H., Akimitsu J. *Phys. Rev. B* **73**, 184422 (2006)
10. Komarek A.C., Roth H., Cwik M., Stein W.-D., Baier J., Kriener M., Boureé F., Lorenz T., Braden M. *Phys. Rev. B* **75**, 224402 (2007)
11. Agzamova P.A., Petrov V.P., Chernyshev V.A., Nikiforov A.E. *Low Temp. Phys.* **41**, 34 (2016)
12. Agzamova P., Nikiforov A., Nazipov D. *J. Low Temp. Phys.* **185**, 544 (2016)
13. Perdew J.P., Ernzerhof M., Burke J. *Chem. Phys.* **105**, 9982 (1996)
14. Adamo C., Barone V. *J. Chem. Phys.* **110**, 6158 (1999)
15. Dovesi R., Orlando R., Erba A., Zicovich-Wilson C.M., Civalieri B., Casassa S., Maschio L., Ferrabone M., De La Pierre M., D’Arco P., Noel Y., Causa M., Rerat M., Kirtman B. *Int. J. Quantum Chem.* **114**, 1287 (2014)
16. Corá F., Alfredsson M., Mallia G., Middlemiss D.S., Mackrodt W.C., Dovesi R., Orlando R. *Struct. Bond.* **113**, 171 (2004)
17. Evarestov R.A. *Quantum Chemistry of Solids*, Springer-Verlag, Heidelberg (2007)
18. Corá F. *Mol. Phys.* **103**, 2483 (2005)
19. Mackrodt W.C., Harrison N.M., Saunders V.R., Allan N.L., Towler M.D., Aprá E., Dovesi R. *Philosoph. Mag. A* **68**, 653 (1993)

20. www.tc.uni-koeln.de/PP/clickpse.en.html
21. Mallia G., Orlando R., Roetti C., Ugliengo P., Dovesi R. *Phys. Rev. B* **63**, 235102 (2011)
22. Gardner J.S., Gingras M.J.P., Greedan J.E. *Rev. Mod. Phys.* **82**, 53 (2010)
23. Troyanchuk I.O. *Inorg. Mater.* **26**, 182 (1990)
24. Soderholm L., Greedan J.E. *Mat. Res. Bull.* **17**, 707 (1982)
25. Ohama T., Yasuoka H., Isobe M., Ueda Y. *J. Phys. Soc. Jap.* **66**, 3008 (1997)
26. Ohama T., Isobe M., Ueda Y. *J. Phys. Soc. Jap.* **69**, 1574 (2000)
27. Takeda H., Itoh M., Sakurai H. *Phys. Rev. B* **86**, 174405 (2012)
28. Stone N.J. *Atomic Data and Nuclear Data Table* **111-112**, 1-28 (2016)
29. Ichikawa H., Kano L., Saitoh M., Miyahara S., Takeda M., Hirota K. *J. Phys. Soc. Jap.* **74**, 1020 (2005)